

Biofabrication methods for the patterned assembly and synthesis of viral nanotemplates

K Gerasopoulos^{1,2,3}, M McCarthy⁴, P Banerjee^{2,3}, X Fan^{3,5},
J N Culver⁶ and R Ghodssi^{1,2,3,5}

¹ MEMS Sensors and Actuators Laboratory (MSAL), University of Maryland, College Park, MD 20742, USA

² Department of Materials Science and Engineering, University of Maryland, College Park, MD 20742, USA

³ Institute for Systems Research, University of Maryland, College Park, MD 20742, USA

⁴ Department of Mechanical Engineering, Massachusetts Institute of Technology, Cambridge, MA 02139, USA

⁵ Department of Electrical and Computer Engineering, University of Maryland, College Park, MD 20742, USA

⁶ Center for Biosystems Research, University of Maryland Biotechnology Institute, MD 20742, USA

E-mail: ghodssi@umd.edu

Received 19 November 2009, in final form 22 November 2009

Published 6 January 2010

Online at stacks.iop.org/Nano/21/055304

Abstract

This paper reports on novel methodologies for the patterning and templated synthesis of virus-structured nanomaterials in two- and three-dimensional microfabricated architectures using the *Tobacco mosaic virus* (TMV). The TMV is a high aspect ratio biological molecule which can be engineered to include amino acids with enhanced binding properties. These modifications facilitate self-assembly of the TMV onto various substrates and enable its use as a template for the synthesis of nanostructured materials. This work focuses on the combination of this bottom-up biologically inspired fabrication method with standard top-down micromachining processes that allow direct integration of the virus-structured materials into batch-fabricated devices. Photolithographic patterning of uncoated as well as nickel-coated TMV nanostructures has been achieved using a lift-off process in both solvent and mild basic solutions and their assembly onto three-dimensional polymer and silicon microstructures is demonstrated. In addition to these patterning techniques, *in situ* formation of metal oxide TMV coatings in patterned microfabricated environments is shown using atomic layer deposition directly on the nickel-coated viruses. The biofabrication 'process toolbox' presented in this work offers a simple and versatile alternative for the hierarchical patterning and incorporation of biotemplated nanomaterials into micro/nanofabrication schemes.

(Some figures in this article are in colour only in the electronic version)

1. Introduction

A highly desirable requirement for the incorporation of nanomaterials in practical technological applications is mass production at low cost as well as the ability to accurately control their properties and arrange them in a highly ordered fashion within a functional device.

Conventional synthesis approaches such as vapor-liquid-solid reactions using catalytic particles, epitaxial methods, electrodeposition, sol-gel and hydrothermal synthesis as well as patterning techniques based on porous templates, e-beam and conventional lithography often have to balance the trade-off between good control over materials properties, variability and compatibility with successive fabrication steps on one hand

and reduced cost on the other [1, 2]. Interestingly, nature offers unique traits for materials synthesis based on novel functionalities that can be imparted on biological structures such as proteins, DNA and viruses. Characteristic attributes of templating approaches that utilize biological building blocks to guide the assembly of inorganic materials include low cost and structural versatility of the biologicals, inherent self-assembly properties, the existence of functional groups that catalyze particle growth and the ability to tune their structure through genetic modifications [3].

Among these biological molecules, plant and bacteria viruses have attracted notable interest for bionanotechnology applications. In addition to their self-assembly and tunability properties, they show exceptional stability in a wide range of temperatures and pH values and have even been reported to withstand treatment in solvent-water mixtures [4]. Representative examples of biotemplated viral engineering have been achieved with the M-13 bacteriophage virus which has been genetically modified through phage display techniques to include specific peptides for inorganic material binding and nanoparticle fabrication [5]. In this work, we focus on the *Tobacco mosaic virus* (TMV), a rigid rod consisting of about 2130 identical coat protein subunits stacked in a helix around a single strand of plus sense RNA, leaving a 4 nm diameter channel through the 300 nm long virion axis. The TMV is one of the best-studied viruses and has been extensively used in nanowire fabrication [6]. Previous work by our team has utilized engineered mutations of the TMV to improve coating uniformity of nano-sized particles; more specifically, efficient templates have been achieved through the introduction of one (TMV1cys) or two (TMV2cys) cysteine residues within the virus coat protein open reading frame. Cysteines are amino acids with thiol groups that show enhanced metal binding properties based on strong, covalent-like interactions. Using this methodology, TMV-based wires coated with gold, silver, palladium, platinum, cobalt, nickel as well as multilayer structures of metal–silica–metal particles have been synthesized and shown to self-assemble in a vertical orientation onto gold surfaces [7]. The feasibility of using these coated nanostructures in functional microfabricated devices has been previously demonstrated through the development of a TMV-based nickel–zinc microbattery [8].

While considerable progress has been achieved in the synthesis of nanomaterials based on biological templates, their integration into high-throughput manufacturing processes is still a concern. Reported approaches include scanning probe and dip-pen nanolithography techniques that utilize cantilever tips to transfer molecules of interest to a substrate through capillary and chemical interactions [9]. Salaita *et al* demonstrated a novel variation of this technique where 55 000 such tips can be used for parallel patterning thus addressing the time limitation needed for processing [10]. Selective placement of DNA nanowires has been achieved through self-assembly and functionalization with chemical groups as well as DNA hybridization [11]; this approach has been previously utilized by our group to selectively assemble fluorescently-tagged TMV onto a chitosan-functionalized electrode [12]. An alternative method was presented by Kuncicky *et al* who

demonstrated long-range alignment of TMV conductive fibers by dragging a meniscus of virus suspension on substrates with controlled wettability [13]. Viruses and proteins have also been arranged on substrates through micro-contact printing [14]. This technique uses an elastomeric structure fabricated through soft-lithography which is then wetted with the functional material and stamped on the target substrate. Alternatively, the stamping process has been used to selectively pattern polyelectrolyte multilayers on which viruses can successively assemble [15]. Notwithstanding individual advantages of these methods, they often require special surface treatment (either the target substrate or intermediate layer) which makes them sensitive to processing conditions; they cannot always be scaled up at the wafer level or show compatibility with batch fabrication, attributes very important for large-scale production and device integration.

The work presented in this paper describes a simple and versatile approach for the selective patterning of both metal-coated and uncoated TMV using a lift-off process. The technique requires a single photolithography step and is readily achieved at the wafer level. Additionally, unlike most reported methodologies, the TMV self-assembly and patterning is also performed onto complex out-of-plane microfabricated geometries. Finally, the robustness of the coated TMV is utilized for the *in situ* synthesis of high surface area vertically-assembled core/shell TMV–nickel/metal oxide nanomaterials using an atomic layer deposition (ALD) coating step, thus expanding the toolbox of available chemistries that can be combined with the viral template. The patterning methodologies and structures presented in this paper are currently integrated by our team in projects that utilize the TMV template as a building block. These include selective patterning of virus receptor layers for gas sensing applications, structuring and patterning of nanostructured Li-ion battery electrodes, and development of hierarchical structures for superhydrophobic and superhydrophilic surfaces; results from these investigations will be the focus of future publications.

2. Experimental methods

2.1. Materials

Silicon wafers (p-type, 4 inch, <100> test grade) were purchased from Silicon Quest Int. (NV, USA). Photoresists Shipley 1813 and SU-8 50 and developers Microposit 352 and SU-8 developer were purchased from Microchem (MA, USA). Photoresists AZ5214 and AZ9245 and developer AZ400K were purchased from MaysChem (IN, USA). Sodium tetrachloropalladate (NaPdCl₄, 98%), nickel (II) chloride hexahydrate (NiCl₂, 99%), sodium tetraborate (Na₂B₄O₇, 99%), dimethylamine borane (DMAB, 97%), were purchased from Sigma Aldrich (MO, USA). Glycine (tissue Grade) was purchased from Fischer Scientific (PA, USA). 10 ml of 10 mM Pd catalyst solution was prepared by dissolving 29.419 mg of NaPdCl₄ in de-ionized (DI) water. Nickel plating solution (25 ml) was prepared by mixing 0.6 g NiCl₂, 0.45 g Glycine, 1.5 g Na₂B₄O₇, 0.77 g DMAB and DI water and stirring until the pH of the solution becomes 7. TMV1cys was

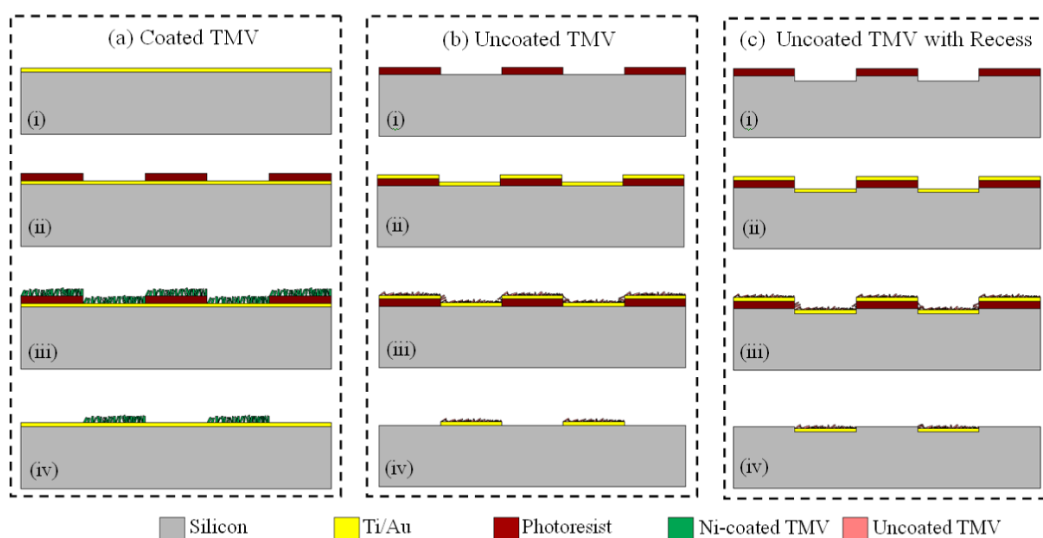


Figure 1. Schematic representation of the lift-off patterning processes for nickel-coated TMV (a), uncoated TMV (b) and uncoated TMV with an etched recess—(a). Coated TMV: e-beam evaporation of Ti/Au (i), photolithography with positive or negative photoresist (ii), TMV assembly and Ni coating (iii) and removal of photoresist in acetone (iv). (b) Uncoated TMV: photolithography with positive photoresist (i), Ti/Au evaporation (ii), TMV assembly (iii), lift-off of Au and TMV in a developer mixture or acetone (iv). (c) Uncoated TMV. After photolithography, a shallow recess ($1 \mu\text{m}$) is etched using DRIE (i), steps (ii)–(iv) are identical.

prepared purified according to standard previously reported methodologies [16, 17].

2.2. TMV patterning

The basic concept of the TMV photolithographic patterning is derived from the conventional lift-off process that is used in the MEMS and semiconductor industry to pattern metallization lines. Photoresist is used to transfer the desired features from an optical mask onto the wafer which is then immersed into a pH 7 phosphate buffer (PBS) solution containing the virus. After TMV self-assembly on the substrate, the photoresist is removed in a solvent or developer solution, leaving TMV only on the patterned surfaces. Depending on the type of TMV nanostructure that has to be patterned (uncoated TMV1cys or nickel-coated TMV1cys), this general approach is modified accordingly to facilitate processing as well as characterization of the samples using high resolution microscopy techniques. Both methodologies are shown schematically in figure 1 and described in detail in the following subsections.

2.2.1. Nickel-coated TMV patterning. The fabrication begins with evaporation of titanium and gold metal layers on a p-type 4 inch silicon wafer to thicknesses of 10 and 50 nm respectively. This step is followed by photolithography using an optical mask that contains various features (lines, squares and circles) with size and spacing ranging from $100 \mu\text{m}$ down to $2 \mu\text{m}$; this is the minimum feature size that can be obtained from the mask manufacturer for contact alignment. Both positive and negative photoresists (Shipley 1813 and image-reversed AZ5214 respectively) with varying thicknesses were employed. For Shipley 1813, the wafer was exposed in a contact aligner (Quintel Q-4000) with a dose of 180 mJ cm^{-2} and developed for 30 s in Microposit 352. When AZ514 was

used, the wafer was exposed with the mask at 40 mJ cm^{-2} , post-exposure baked at 125°C for 45 s and then flood-exposed (no-mask) at 2000 mJ cm^{-2} to invert the polarity. Development was performed in a mixture of AZ400K developer and water in a 1:6 ratio for 2 min. After development, the three-step viral self-assembly and nickel coating process is performed on cleaved chips as previously described [8]. The chips are placed in a TMV-containing sodium phosphate buffer solution at a virus concentration of 0.1 mg ml^{-1} and allowed to incubate overnight. After TMV self-assembly, the die are immersed for a few hours in a palladium catalyst solution prepared by mixing a palladium salt (sodium tetrachloropalladate) with PBS (ratio of 1:10 to 1:15) and finally they are coated with nickel in an electroless plating solution in which they are immersed for 3–5 min. The metallization step is followed by treatment of the samples in an acetone bath using ultrasonication.

2.2.2. Uncoated TMV patterning. The process begins with the photolithography step using Shipley 1813 as the positive resist on a 4 inch silicon wafer with the same optical mask. The photoresist is exposed for 15 s under UV light and then developed with Microposit 352. After development, the wafer is flood-exposed for 30–40 s to allow lift-off in the developer solution. Before metallization, some of the wafers are shallow-etched with Deep Reactive Ion Etching (DRIE) to a depth of approximately $1 \mu\text{m}$ (figure 1(c)); this small fabricated recess was expected to accelerate the lift-off process and was investigated for comparison with the standard method. E-beam evaporation is then used to deposit thin films of titanium (10 nm) and gold (50 nm) on the wafer. Finally, the wafer is cleaved and the individual chips are immersed in the TMV-containing solution (concentration of $\sim 0.1 \text{ mg ml}^{-1}$) and allowed to incubate overnight.

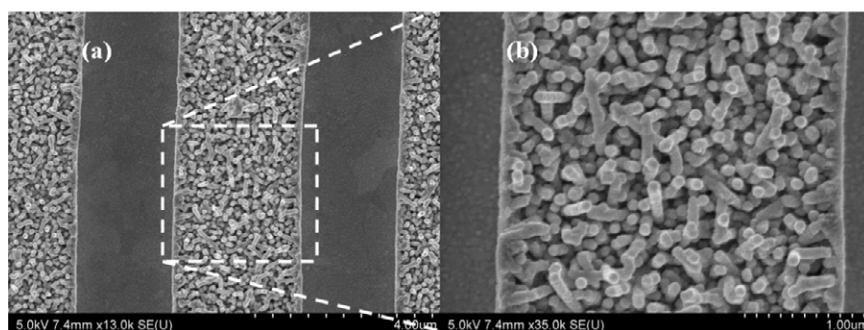


Figure 2. SEM images of patterned nickel-coated TMV features; (a) microfabricated virus-coated lines with size and spacing of $2\ \mu\text{m}$ and (b) close-up view of the textured surface.

2.3. Three-dimensional microstructure fabrication

Silicon structures were etched in the STS with a rate of $3\ \mu\text{m}\ \text{min}^{-1}$ to a depth of $240\ \mu\text{m}$. The etching mask was a $5.5\ \mu\text{m}$ thick AZ9245 photoresist. The resist was spun at speeds of 1750 rpm for 5 s and 3000 rpm for 40 s and soft-baked at $110\ ^\circ\text{C}$ for 90 s. The wafer was exposed at a dose of $300\ \text{mJ}\ \text{cm}^{-2}$ and developed in a mixture of AZ400K and DI water in a 1:3 ratio. After etching, photoresist was removed in acetone and layers of chrome (50 nm) and gold (250 nm) were sputtered on the substrate in an AJA sputtering unit. The polymer structures were fabricated on silicon wafers which were cleaned in acetone, methanol, isopropyl alcohol and DI water in ultrasonics and dehydrated at $200\ ^\circ\text{C}$ for 20 min. SU-8 50 was spun at speeds of 600 rpm and 2500 rpm and soft-baked at $75\ ^\circ\text{C}$ with a ramp of $300\ ^\circ\text{C}\ \text{h}^{-1}$ for 50 min. Exposure was performed in the aligner for 80 s and post-exposure bake followed under the same conditions as the soft-bake. The wafer was finally developed in SU-8 developer for 10 min with agitation.

2.4. Synthesis of core/shell nickel/metal oxide nanostructures using ALD

The nickel-coated patterned chips were placed in a TFS 500 BENEQ™ ALD reactor. The deposition of Al_2O_3 was performed using alternate pulse sequences of trimethyl aluminum (TMA) and H_2O at $220\ ^\circ\text{C}$ while the deposition of TiO_2 utilized tetrakis-dimethyl amido titanium (TDMAT) and H_2O at $150\ ^\circ\text{C}$. The measured deposition rate for these recipes has been determined to be $0.1\ \text{nm}/\text{cycle}$ for Al_2O_3 and $0.05\ \text{nm}/\text{cycle}$ for TiO_2 , close to reported values in literature [18]. The target thickness for both the deposited layers was kept to be 30 nm to enable observation of a notable change with the electron microscopy imaging techniques.

2.5. Characterization

SEM images were obtained using a Hitachi SU-70 Analytical UHR FEG-SEM. AFM analysis was done using a Digital Instruments DI-300 atomic force microscope in tapping mode. TEM analysis was done with a JEOL JEM 2100 TEM while EDS was performed with an Oxford INCA 250 system attached to a JEOL JEM 2100F TEM/STEM. The TEM samples were prepared as follows: chips for TEM analysis were

prepared on a freshly-cleaved mica substrate where a thin layer of gold has been thermally evaporated to serve as a base for TMV assembly. The ALD-TMV-coated mica substrates were first dehydrated in 70%, 95% and 100% (2 times) acetone for 10 min each time. Spurr's resin was prepared as suggested in [19] and the chips were immersed in mixtures of acetone:Spurr's at ratios of 1:1, 1:2 and 1:3 for 30 min each time. After immersion in 100% Spurr's for 1 h, the chip was embedded in Spurr's and the resin was polymerized overnight at $70\ ^\circ\text{C}$ in an oven. Thin sections (70 nm) were obtained with a diamond knife and mounted onto carbon/formvar coated TEM grids.

3. Results and discussion

3.1. Nickel-coated TMV

The patterning approach for the TMV-templated metallic nanostructures is simple and straightforward due to the remarkable robustness of coated viruses in solvents as well as the ability to characterize the samples directly using scanning electron microscopy (SEM). Immersion of the photoresist-patterned nickel-coated chips in an acetone bath followed by ultrasonication results in lift-off of the underlying photoresist layer leaving the nickel-coated viruses onto the patterned surfaces. Figure 2 shows SEM images of the minimum patterned feature size including a close-up view of the textured surface. The SEM images demonstrate that nickel-coated TMV-structured lines with size and spacing as small as $2\ \mu\text{m}$ can be clearly resolved. It is also observed that the metal coating enables nanoscale three-dimensional assembly of the otherwise flat-laying virus resulting in very high surface area patterns. This near-vertical assembly has been explained in detail in previous publications [7, 8] and it is very important in applications such as battery electrodes and fuel cell catalysts where maximum surface area is desirable. The patterning methodology investigated using this lift-off technique is independent of the photoresist polarity or thickness and it is limited only by the minimum mask feature size. While the concept has been demonstrated using nickel coating, the process has also been successfully combined with other similar solution-based coating recipes that were developed by our group. This versatility and simplicity make it a very promising candidate for large-scale manufacturing of nanostructured templates.

3.2. Uncoated TMV

Two important considerations had to be taken into account when developing the fabrication process for the uncoated TMV. First of all, extensive treatment of the virus in solvents (commonly used solutions for photoresist removal) can result in structural destabilization of the TMV or other peptides that could be potentially attached on the virion surface; this led to the investigation of alternative methods to remove the polymer masking layer based on less reactive solutions. The second requirement is pertinent to the sample characterization which is conducted with both SEM and atomic force microscopy (AFM) in this experiment so that nanoscale structural effects can be analyzed. Uncoated TMV cannot be viewed with an optical microscope and this necessitates the use of 'alignment marks' to achieve correct placement of the AFM tip on patterned and unpatterned areas. The first concern is addressed by employing positive photoresist during photolithography, since this type can be treated with UV light after fabrication and removed with both solvent and developer mixtures. To facilitate imaging, the base gold layer for TMV assembly is deposited after photoresist patterning (as in standard lift-off) so that discrimination between patterned structures can be made easily.

Two lift-off methodologies utilizing photoresist developer and an acetone solution were investigated. The developer is a highly basic solution (pH 13–14) consisting of sodium hydroxide, sodium tetraborate, boric acid and water; for this application, it was mixed with sodium phosphate buffer (0.1 M, pH 7) at ratios of 1:3 and 1:5 which resulted in a decrease in the pH of the mixture to values of ~ 9 and ~ 8 respectively. These milder conditions were necessary to avoid destabilization of the virus structure. The chips were immersed in the solution and placed on a hotplate heated at 55 °C to accelerate the photoresist removal process. This temperature was selected again based on literature findings regarding the virus stability in certain temperature ranges [8]. Lift-off in acetone was more straightforward and involved immersion of the die in the solvent at room temperature. In both cases, slight manual agitation was applied periodically to assist the process. The developer-based process was, as expected, slower and required 5–7 h for patterning of features down to 10 μm . Smaller features required treatment up to 30 h to be completely resolved and partial structural destabilization was observed for such long process times. In all cases, continuous agitation accelerated the lift-off rate. On the other hand, gold/virus lift-off in acetone proceeded at a faster pace (1–2 h for similar feature sizes). It was also observed that in the wafers without the shallow-etched trenches photoresist removal was even slower. After completion of the process, the samples were rinsed in DI water and dried on a hotplate at 40 °C.

Figures 3(a) and (e) show optical images of chips patterned in the developer mixture (1:5) and acetone respectively. It can be clearly seen that gold features have been lifted off from the silicon substrate. The nanostructure of the patterned surfaces was investigated using an atomic force microscope. Figures 3(b) and (f) show height scans of untreated TMV surfaces on gold substrates which were used

as control while figures 3(c), (g), (d) and (h) are scans of gold and silicon areas from the samples of figures 3(a) and (e) respectively. In all images it is seen that, unlike the case of the metal-coated TMV, the viruses lay flat on the substrate as a result of the drying process since there is no coating layer to provide the three-dimensional support. The interface between the gold and silicon surfaces on chips patterned using developer mixed with PBS in a 1:3 ratio and acetone are shown in figure 4 where the selectivity in TMV patterning is clearly demonstrated. By comparing the untreated and developer-patterned surfaces it can be observed that the mild-pH lift-off process does not affect the virus structure when the dilution is performed in the range of 1:3 to 1:5. On the other hand, samples treated in the solvent solution show a different morphology compared to the untreated TMV as evident from the height scan in both the gold and silicon areas as well as the height and phase images of figure 4 that show additional virus fragments on the surface. This is attributed to precipitation of the coat proteins in acetone which results in unfolding as well as fracturing of the virus particles and successive irregular assembly across the chip area.

The post-patterning chemical functionality of the uncoated TMV was investigated for both techniques by attempting metallization of the structures. Optical microscope inspection was employed to determine that the gold areas were removed from the silicon substrate. Once successful photoresist removal was verified, the samples were gently rinsed in a PBS solution without prior drying and then metallized with nickel using the two-step process described earlier. Figures 5(a) and (b) show characteristic SEM images of chips patterned in developer (5:1) and acetone respectively. It is observed in both cases that the TMV is successfully metallized. In the developer-processed specimens a small number of fragments were found in the silicon areas, which could be due to re-deposition of solution-excess viruses during the lengthy process. This effect is more pronounced however when TMV is immersed in acetone as was indicated in the AFM analysis as well. In addition to cases of TMV fragments, poor coverage of the substrates was occasionally observed in acetone.

In conclusion, two lift-off methodologies for the patterning of uncoated TMV on microfabricated structures have been successfully developed. The developer-based process is lengthy as several hours are required to resolve virus-coated structures as small as 10 μm however no structural degradation or difference in morphology compared to untreated surfaces has been observed during these times. When the process is performed in acetone, features are lifted off faster but negative effects on the virus structure have been noticed with variability even on the same substrate. Since post-patterning chemical functionality is maintained, depending on the requirements of a specific process, the most suitable of the two techniques can be adopted.

3.3. Assembly of coated TMV on three-dimensional geometries

Assembly of high aspect ratio nanostructures on three-dimensional microstructures is a very attractive approach

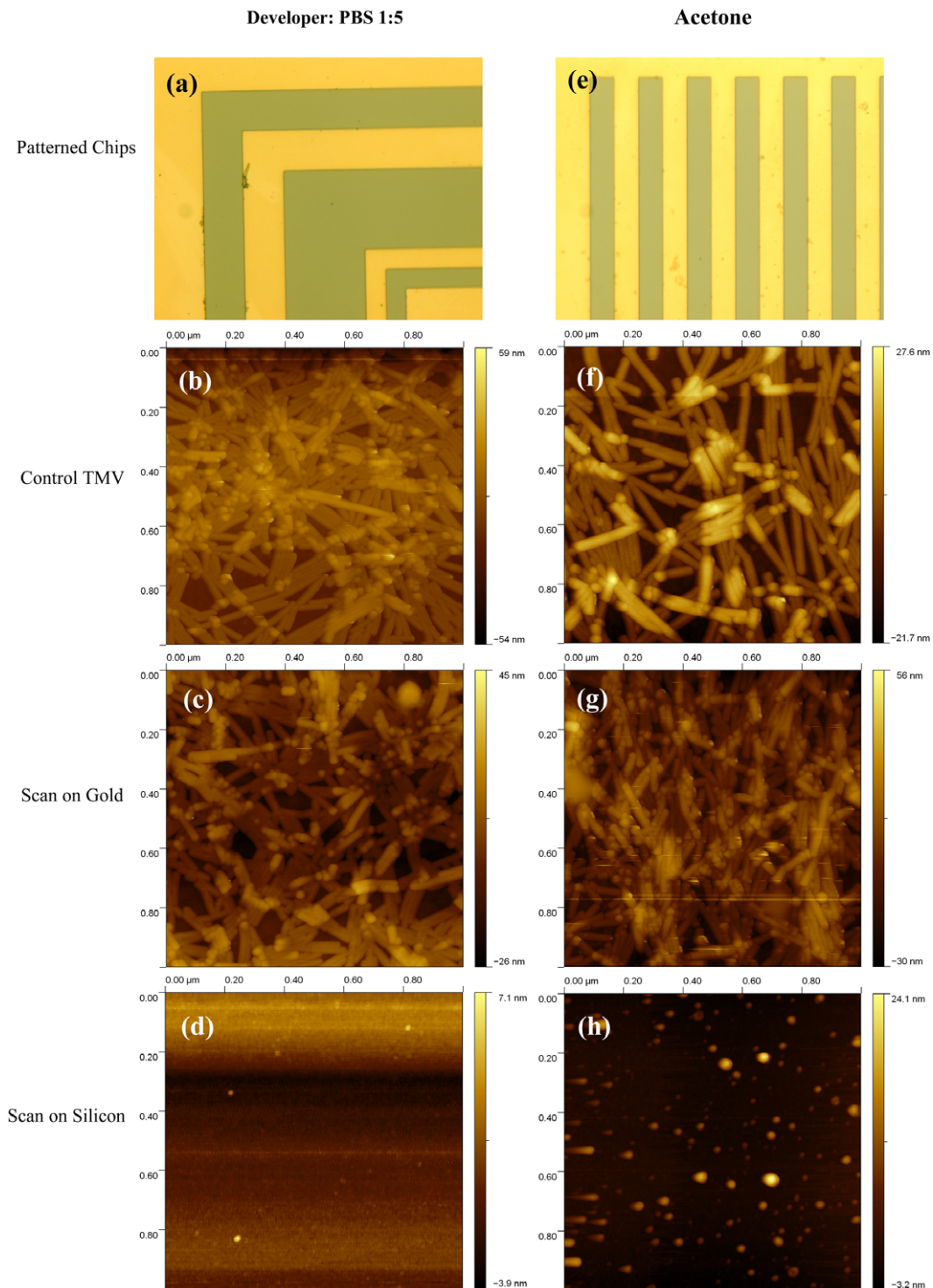


Figure 3. Images of TMV coated chips patterned in developer:buffer 1:5 mixture (left column) and acetone (right column) ((a), (e)) optical images of chip surface showing that coated gold has been removed selectively, ((b), (f)) AFM height scans of an untreated control surface cleaved from the same substrate before immersion in the respective patterning solution, ((c), (g)) AFM height scans of the gold surfaces of figures (a) and (e) and ((d), (h)) AFM height scans of the silicon surfaces of (a) and (e). The AFM images have been obtained over $1 \mu\text{m} \times 1 \mu\text{m}$ areas and the height scale is given in nm.

in applications where increased surface area in the out-of-plane dimension is particularly beneficial, such as microfluidic wicking structures and active battery electrodes. The self-assembly properties of the virus in simple solution-based reactions and the functional groups on its surface enable the

integration of the TMV-templated materials into such complex architectures. Two methods were investigated to demonstrate the feasibility of this three-dimensional assembly; the first method is a direct extension of the in-plane biofabrication and utilizes silicon substrates etched using DRIE and sputtered

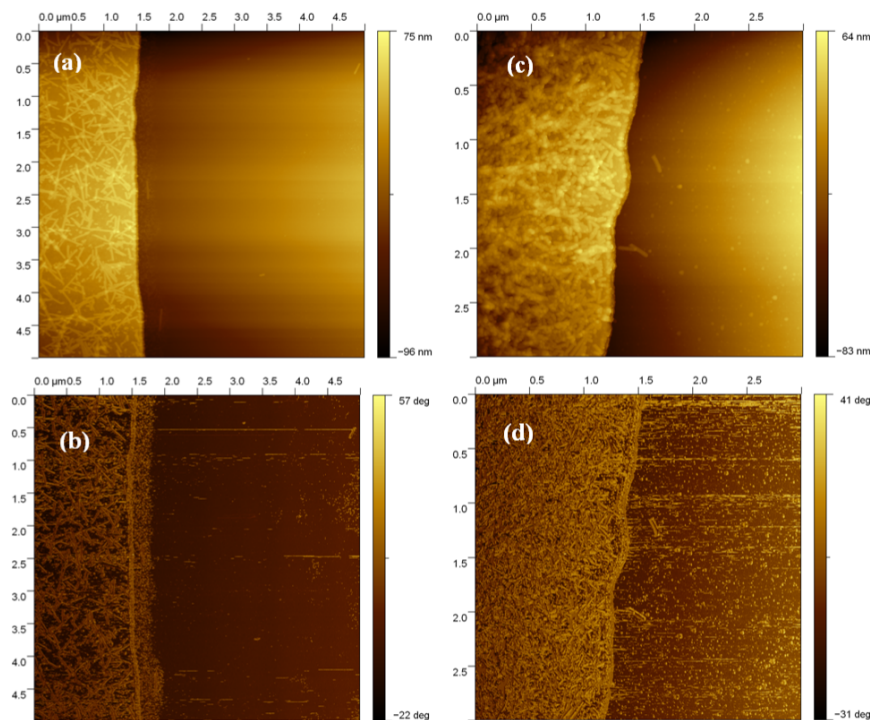


Figure 4. AFM height scans of the interface between gold and silicon of chips patterned in a 1:3 developer/buffer mixture (a) and acetone (c). Figures (b) and (d) show the phase mode AFM scans for (a) and (c) respectively.

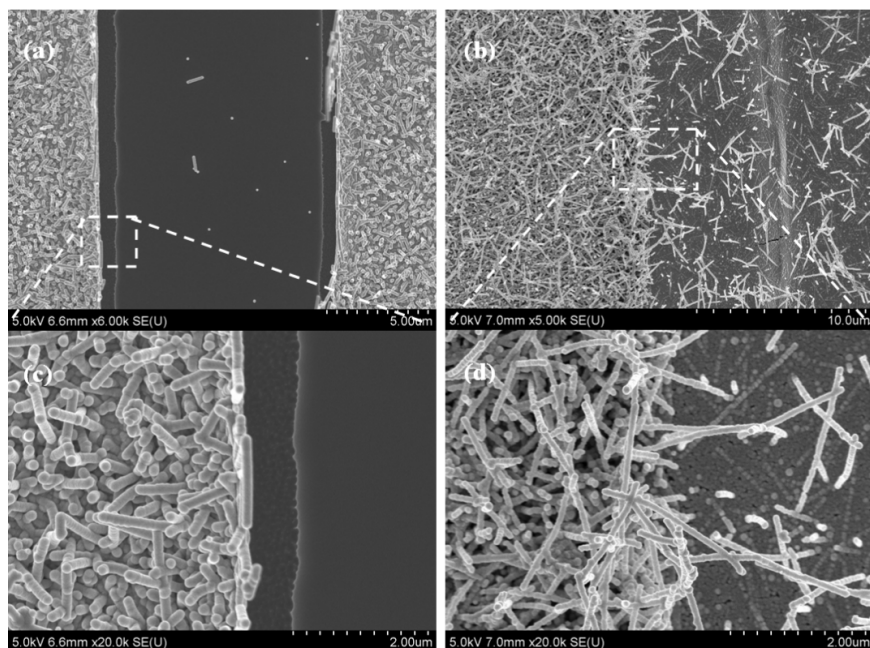


Figure 5. SEM images of TMV that was first patterned in 5:1 buffer:developer mixture (a) and acetone (b) and then coated with nickel to verify post-patterning chemical functionality. Images (c) and (d) show close-up views of the textured surfaces.

with metal layers. The second process was inspired by findings of our previous work, where it was observed that TMV adheres to polymers as well [8]. Here, SU-8 is employed for the fabrication of microstructured surfaces on which assembly of the nickel-coated viruses is achieved.

Following the microfabrication processes described in section 2, individual chips from both wafers were coated with

TMV and nickel. SEM images of the coated substrates as well as close-up views of the textured surfaces are shown in figure 6. The mechanism that enables TMV attachment onto SU-8 has not been clearly defined. The effect of the cysteine mutation was investigated by the addition of diethyl-triethol (DTT) to the virus solution, a chemical that can impede the functionality of the cysteine amino acid. Little or no difference was observed

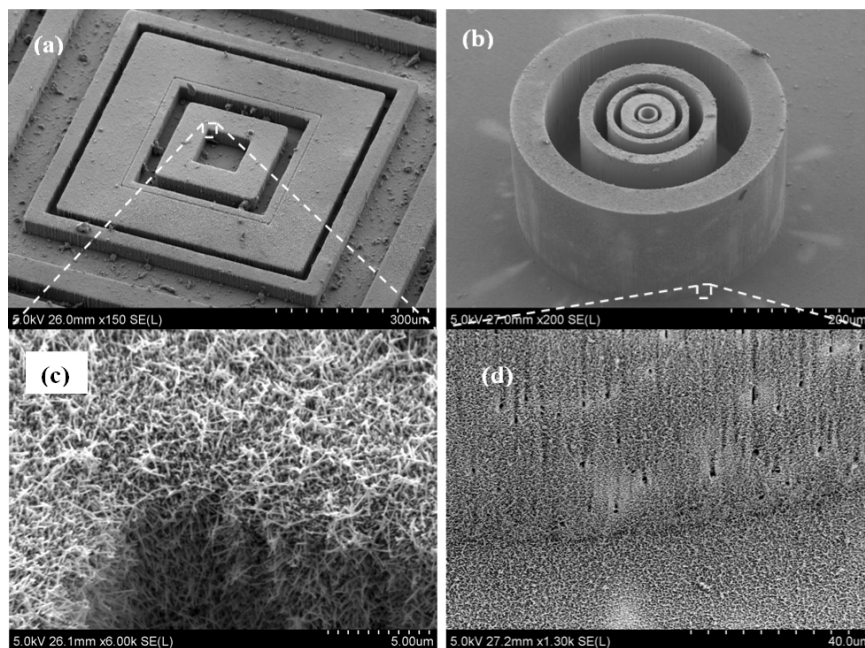


Figure 6. SEM images of three-dimensional microstructures covered with nickel-coated TMV, (a) SU-8 structures, (b) structures etched in silicon. Bottom pictures (c) and (d) show exploded views of the textured surfaces outlined by the dotted areas in (a) and (b).

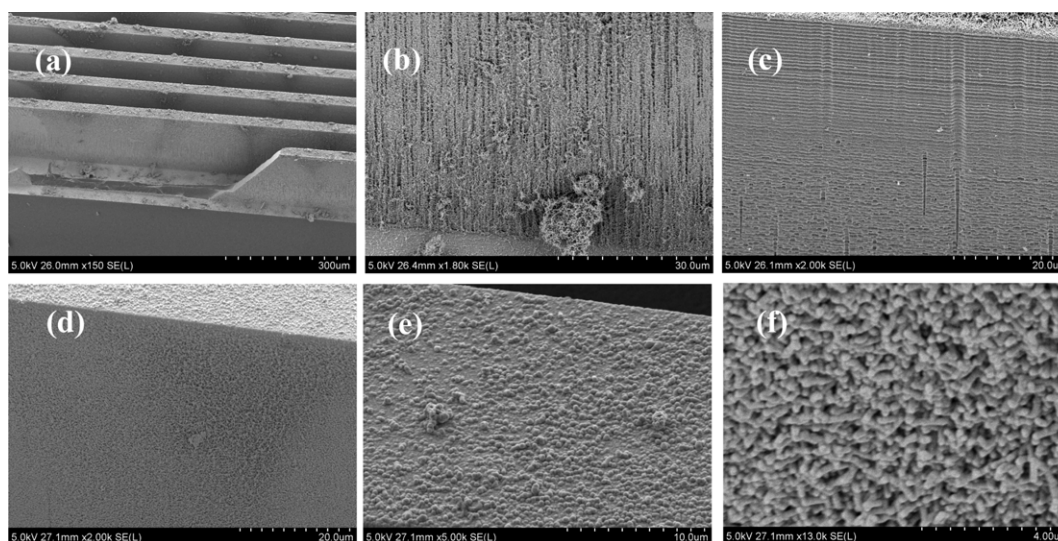


Figure 7. (a) Cleaved high aspect ratio structures in silicon, examples of (b) uniformly covered sidewall and (c) poorly covered sidewall; (d) a similar structure coated with constant stirring of solutions; close-up views of top (e) and sidewall (f) surfaces of the structure shown in (d).

however in the density of the coated TMV on SU-8 after this treatment, indicating that the engineered cysteine residues do not play a direct role in SU-8 attachment.

Comparison of these two processes indicates that, while silicon etching allows the realization of higher aspect ratio structures than SU-8 and can be used in applications where a conductive substrate is required, sidewall coverage was not as consistent as in the polymer case. More specifically, cases were identified in the silicon structures where both interior sidewalls and bottom surfaces (in between features) were not as densely coated as other similar features even on the same chip (figures 7(a)–(c)). Similar variability was not seen in SU-8.

These observations indicate that diffusion of the liquid through the high aspect ratio structures as well as insufficient gold coverage and difference in wettability of the gold-sputtered silicon and SU-8 surfaces must be among the causes for this inconsistency.

The effect of liquid diffusion and surface wettability was investigated by stirring the TMV and electroless plating solutions. This was achieved by placing the chips vertically inside a 10 ml beaker with the aid of a three degree of freedom stage and placing the assembly on a hotplate to provide magnetic actuation. It was observed that stirring results in consistently denser sidewall coverage; however, fragmentation

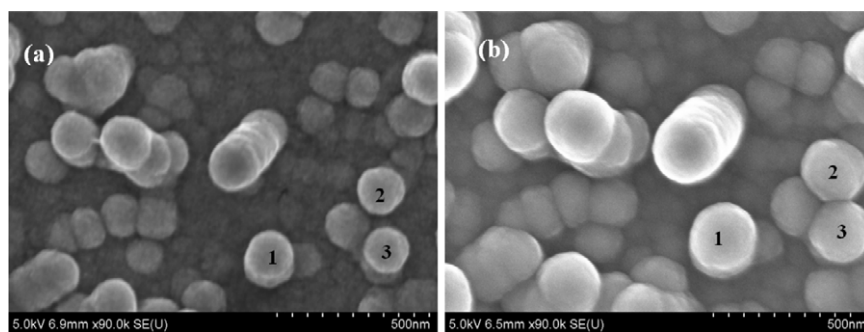


Figure 8. SEM images of patterned nickel-coated TMV structures before (a) and after (b) ALD coating of TiO_2 —the diameter of particles 1–3 has been measured using ImageJ software to be 151, 149, 144 nm in (a) and 214, 206, 197 nm in (b).

of the TMV especially on the exposed top surfaces was a negative side effect (figures 7(d)–(f)). Based on these results, better utilization of the silicon structures can be achieved by using coatings that can decrease surface tension, adopting alternative geometries (e.g. cylindrical posts) or by adjusting the lateral distance between structures such that liquid can easily access all features of interest.

3.4. *In situ* core-shell nanostructure synthesis using ALD

The diverse nature of nanomaterial applications requires the existence of templates that can be versatile and allow synthesis of a broader range of functional surfaces. The previously developed templating methodologies have been limited to the use of electroless plating reactions for the decoration of TMV with inorganic particles. Utilizing these metallic templates other micro/nanofabrication approaches can be integrated into TMV-based materials synthesis. ALD is a unique deposition method that is ideally suited for uniform coating of high aspect ratio surfaces. In this work, the feasibility of conformal deposition of materials onto the nickel-coated TMV surface was investigated. Two established recipes for aluminum oxide (Al_2O_3) and titanium oxide (TiO_2) were used as a proof-of-concept demonstration; however, this method can be expanded to include any material that can be deposited using ALD.

Samples for ALD deposition were prepared using the photolithographic patterning technique described in section 3.1. The utilization of patterned chips was preferred over plain nickel-coated surfaces because it provides consistent locations for SEM characterization before and after deposition. In this experiment, a lower concentration of TMV1cys was selected, typically 0.05 or 0.075 mg ml^{-1} . At lower concentrations, the packing density of the nanostructured materials is decreased and this facilitates easier imaging of individual virus particles. SEM images of nickel-coated TMV surfaces before and after deposition of 30 nm of TiO_2 are shown in figure 8. Comparison of the rod diameters on the marked vertically-aligned particles 1–3 shows an increase after the ALD process. This increase has been estimated using ImageJ software to be on the order of 30 nm, which was the intended thickness based on the processing parameters.

The coating uniformity was further investigated using cross-sectional transmission electron microscopy (TEM). Figures 9(a) and (b) show the side and bottom view of an

individual TMV particle while figures 9(d)–(f) contain the corresponding energy-dispersive x-ray spectroscopy (EDS) data of the particle in the inset (figure 9(c)). Oxygen is present due to both the Al_2O_3 as well as nickel that has been oxidized. The absence of any signal from nickel until approximately ~ 25 nm indicates the excellent coating uniformity of the alumina layer.

ALD has been previously employed by other researchers for TMV coating. Knez *et al* demonstrated a room temperature deposition process for the decoration of TMV with layers of alumina and titania [20]. In the work presented here, two significant advancements have been achieved. Deposition of composite materials on the nickel-coated virus surface expands the toolbox of available processes since the structure of the virus is entirely protected by the thin metal coating thus allowing higher-temperature recipes to be applied without structural degradation of the virus. Tuning of the layer thicknesses is also possible by adjusting the deposition parameters for electroless plating and ALD steps. Additionally, the surface-attaching properties of the cysteine-modified TMV1cys as well as the photolithographic patterning capability enable *in situ* synthesis of the desired materials without any requirement for post-integration in a device or substrate since the ALD and coated TMV lift-off processes could be combined for selective deposition of the films.

4. Conclusion

The development of novel fabrication methodologies for the synthesis and patterning of nanostructured materials using the *Tobacco mosaic virus* was presented in this paper. Metal-coated as well as uncoated TMV have been lithographically patterned using a lift-off process that relies on selective photoresist and metal layer removal from a silicon substrate leaving the viruses on clearly-defined surfaces. Uncoated viruses maintain their chemical functionality after fabrication which was verified through metallization with a thin nickel layer. This fabrication approach is simple as it requires only one photolithography step and no particular surface modification. It is versatile since it can be expanded to multiple virus-templated materials while the wafer level scalability enables integration into high-throughput manufacturing processes. The robustness of the metal-coated TMV templates and their patterning ability has been

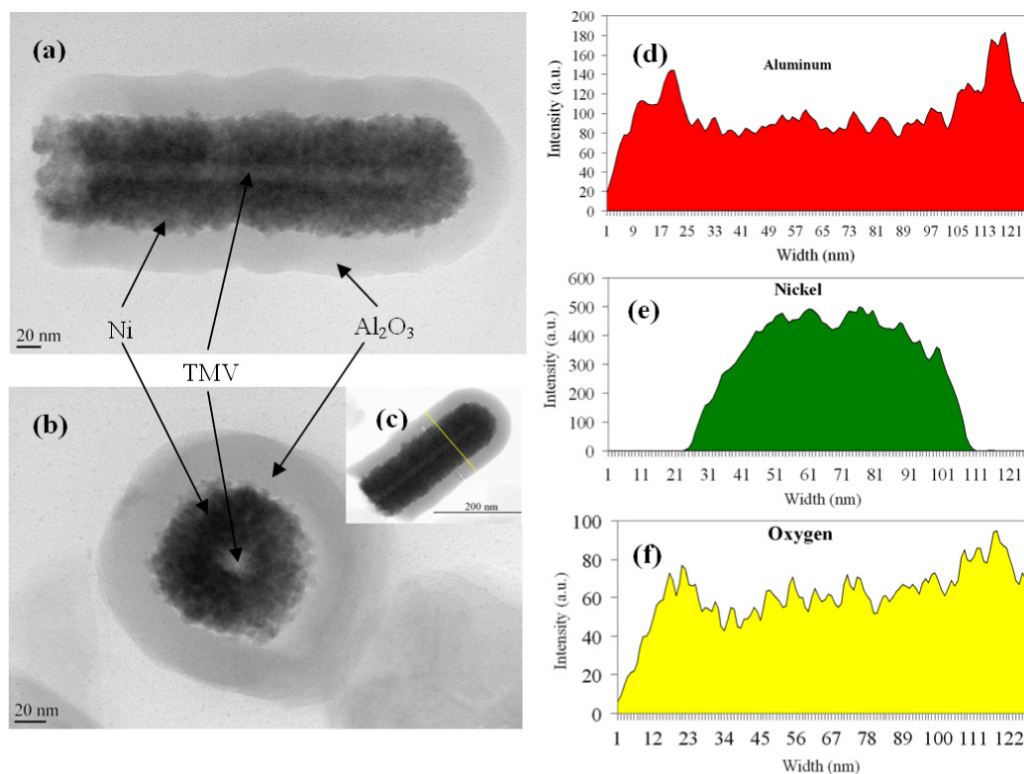


Figure 9. Side (a) and bottom (b) view TEM images of TMV particles coated with layers of nickel (electroless plating) and Al_2O_3 (ALD)—EDS line scan data of the STEM image (c) are shown on the right for the elements of interest (Al, Ni, O). It can be seen that aluminum signal is picked from the start of the line scan (d) while nickel signal is zero until ~ 25 nm (e); this indicates that the first coating layer is due to ALD of Al_2O_3 —oxygen (f) is due to both materials.

utilized in the development of two additional processes. The assembly of the nickel-coated nanostructures on three-dimensional microstructures fabricated in silicon and SU-8 was demonstrated. Finally, uniform coating of patterned nickel-coated TMV structures with layers of alumina and titania using an ALD process allows the incorporation of more functional materials in this templating approach through the formation of core/shell TMV–nickel/metal oxide heterostructures. Results from this work demonstrate an alternative route to bridging the worlds of bionanotechnology and microfabrication through the combination of top-down and bottom-up processes. These developed methods will serve as the foundation for efficient integration of templated nanostructures in applications such as high sensitivity and selectivity sensor arrays, complex micro/nanostructures with controlled texture surfaces as well as nanostructured electrodes and catalysts for microfabricated energy storage devices.

Acknowledgments

This work is funded by the Laboratory for Physical Sciences (LPS), Maryland Technology Development Corporation (TEDCO), National Science Foundation—Nanomanufacturing program (NSF-CMMI 0927693) and Department of Energy-Basic Energy Sciences (FG0202ER45975). The authors would like to thank all clean-room staff at LPS and Maryland Nanocenter; also, Mr Tim Mangel at the Laboratory for Biological Ultrastructure and Mr Larry Lai at the Nanoscale

Imaging Spectroscopy and Properties Lab at UMD for assisting with TEM sample preparation and TEM and AFM imaging.

References

- [1] Durrer L, Helbling T, Zenger C, Jungen A, Stampfer C and Hierold C 2008 *Sensors Actuators B* **132** 485
Xiang B, Wang P, Zhang X, Dayeh S A, Aplin D P R, Soci C, Yu D and Wang D 2007 *Nano Lett.* **7** 323
Zhao Y, Jin J and Yang X 2007 *Mater. Lett.* **61** 384
Wang X, Wang X, Huang W, Sebastian P J and Gamboa S 2005 *J. Power Sources* **140** 211
Yue G H, Yan P X, Fan X Y, Wang M X, Qu D M, Yan D and Liu J Z 2006 *J. Appl. Phys.* **100** 124313
- [2] Wang J H, Su P Y, Lu M Y, Chen L J, Chen C H and Chu C J 2005 *Electrochem. Solid-State Lett.* **8** C9
Cui Y, Bjirk M T, Liddle J A, Snnichsen C, Boussert B and Alivisatos A P 2004 *Nano Lett.* **4** 1093
Sharma G, Kripesh V, Kim M C and Sow C H 2007 *Sensors Actuators A* **A139** 272
- [3] Ma N, Sargent E H and Kelley S O 2007 *J. Mater. Chem.* **18** 954
Sotiropoulou S, Sierra-Sastre Y, Mark S S and Batt C A 2008 *Chem. Mater.* **20** 821
- [4] Evans D J 2008 *J. Mater. Chem.* **18** 3746
- [5] Huang Y, Chiang C Y, Lee S J, Gao Y, Hu E L, Yoreo J D and Belcher A M 2005 *Nano Lett.* **5** 1429
Lee S W, Mao C, Flynn C E and Belcher A M 2002 *Science* **296** 892
Mao C, Solis D J, Reiss B D, Kottmann S T, Sweeney R Y, Hayhurst A, Georgiou G, Iverson B and Belcher A M 2004 *Science* **303** 213
- [6] Knez M, Bittner A M, Boes F, Wege C, Jeske H, Maib E and Kern K 2003 *Nano Lett.* **3** 1079

- Knez M, Sumser M, Bittner A M, Wege C, Jeske H, Kooi S, Burghard M and Kern K 2002 *J. Electroanal. Chem.* **522** 70
- Knez M, Sumser M, Bittner A M, Wege C, Weske H, Martin T P and Kern K 2004 *Adv. Funct. Mater.* **14** 116
- Liou W L, Balandin A A, Mathews D M and Dodds J A 2005 *Appl. Phys. Lett.* **86** 253108
- [7] Royston E, Lee S-Y, Culver J N and Harris M T 2006 *J. Colloid Interface Sci.* **298** 706
- Lee S-Y, Royston E, Culver J N and Harris M T 2005 *Nanotechnology* **16** S435
- Royston E, Ghosh A, Kofinas P, Harris M T and Culver J N 2007 *Langmuir* **24** 906
- Royston E, Brown A D, Harris M T and Culver J N 2009 *J. Colloid Interface Sci.* **332** 402
- [8] Gerasopoulos K, McCarthy M, Royston E, Culver J N and Ghodssi R 2008 *J. Micromech. Microeng.* **18** 10
- [9] Cheung C L, Camarero J A, Woods B W, Lin T, Johnson J E and Yoreo J J D 2003 *J. Am. Chem. Soc.* **125** 6848
- Piner R D, Zhu J, Xu F, Hong S and Mirkin C A 1999 *Science* **283** 661
- [10] Salaita K, Wang Y, Fragala J, Vega R A, Liu C and Mirkin C A 2006 *Angew. Chem. Int. Edn* **45** 7220
- [11] Keren K, Krueger M, Gilad R, Ben-Yospeh G, Sivan U and Braun E 2002 *Science* **297** 72
- Rothemund P W K 2006 *Nature* **440** 297
- [12] Yi H, Nisar S, Lee S-Y, Powers M A, Bentley W E, Payne G F, Ghodssi R, Rubloff G W, Harris M T and Culver J N 2005 *Nano Lett.* **5** 1931
- [13] Kuncicky D M, Naik R R and Velev O D 2006 *Small* **2** 1462
- [14] Balci S, Leinberger D M, Knez M, Bittner A M, Boes F, Kadri A, Wege C, Jeske H and Kern K 2008 *Adv. Mater.* **20** 2195
- Bernard A, Renault J P, Michel B, Bosshard H R and Delamarche E 2000 *Adv. Mater.* **12** 1067
- [15] Yoo P J, Nam K T, Belcher A M and Hammond P T 2008 *Nano Lett.* **8** 1081
- [16] Dawson W O, Beck D L, Knorr D A and Grantham G L 1986 *Proc. Natl Acad. Sci.* **83** 1832
- [17] Gooding G V and Herbert T T 1967 *Phytopathology* **57** 1285
- [18] Ott A W, Klaus J W, Johnson J M and George S M 2006 *Thin Solid Films* **498** 1–2
- [19] Spurr A R 1969 *J. Ultrastruct. Res.* **26** 31
- [20] Knez M, Kadri A, Wege C, Gosele U, Jeske H and Nielsch K 2006 *Nano Lett.* **6** 1172